

January 01, 1994

Quantum circuit-theory and measurements on YBaCuO grain-boundary weak-link bridges

H. How

H. Jiang

A. Widom
Northeastern University

C. Vittoria
Northeastern University

Recommended Citation

How, H.; Jiang, H.; Widom, A.; and Vittoria, C., "Quantum circuit-theory and measurements on YBaCuO grain-boundary weak-link bridges" (1994). *Electrical and Computer Engineering Faculty Publications*. Paper 110. <http://hdl.handle.net/2047/d20002281>

Quantum circuit theory and measurements on Y-Ba-Cu-O grain-boundary weak-link bridges

H. How, H. Jiang, A. Widom, and C. Vittoria
 Northeastern University, Boston, Massachusetts 02115
 (Received 5 April 1993)

The quantum system associated with a resistor-shunted weak-link junction circuit may be described in terms of a single Lagrangian. In this representation the degrees of freedom internal to the dissipative energy of the resistor can be systematically separated from the Hamiltonian formulation of the circuit. This allows us to solve the quantum states of the junction while the effects of the resistor on the circuit are included as a Lagrangian multiplier. In this manner the effects of the measuring apparatus or resistor on the quantum state of the junction may be calculable. The calculations are in very good agreement with experiments.

INTRODUCTION

Experimental evidence is accumulating in demonstrating quantum effects in macroscopic bodies such as in Josephson junction devices.¹⁻⁵ The quantum formulation of a Josephson junction has long been established.^{6,7} However, the influence⁸⁻¹² of the measuring apparatus on the observation of a quantum phenomena in such a junction has not been quantitatively estimated, since each observation¹⁻⁵ was based upon the specifics of the coupling between the measuring apparatus and the quantum circuit. Specifically, if we represent the measuring apparatus as an external resistor to the junction, how does it affect the observation of the quantum phenomena in a superconducting microbridge device? In this paper we present a systematic calculational method by which the effects of a resistor on the observation of a quantum phenomena observed¹³ in a simple superconducting circuit are quantitatively estimated. The reader is referred to the observation of the quantum phenomena and the circuit in Ref. 4. The circuit shown in Fig. 1 consists of a load resistor R_L in series with a high- T_c superconducting microbridge. Besides there may be additional contact resistance drop between the junction and ground, represented as R_G . The observation consists of measuring the discreteness of Cooper carries across the junction.

Clearly, the circuit is made up of dissipative and conservative interaction energy terms. The problem is how to separate the dissipative energy terms, as represented by the cumulative loss resistance in the circuit, from the conservative energy terms and still couple them in a consistent manner. We derive a Lagrangian which contains both conservative and dissipative energy terms.¹⁴ From this Lagrangian a Routhian energy expansion is derived. The Hamiltonian of the conservative system, which consists of an ideal Josephson junction and a shunting capacitance, can be derived from the Lagrangian as the Routhian with the (Josephson) phase treated as the canonical variable. After quantizing the Hamiltonian energy eigenvalues of the conservative system is calculated. The resistor is explicitly treated as a Lagrangian multiplier which does not interfere with the computation of the quantum eigenvalues. Therefore, the dissipative part

of the apparatus is formulated together with a quantum object without recourse to a direct consideration of the many degrees of freedom involved in dissipation. This provides us with a convenient comparison between theory and experiments. The comparison was made between the ground state of the quantum system and the charge mode measured¹³ in the experiment and the comparison is reasonable.

THEORETICAL FORMULATION

We consider the Lagrangian of a singly connected superconducting weak link. An external ac voltage source $V_0 \cos \omega t$ is fed into a load resistor R_L in series with a weak link. The weak link is represented by a conventional resistively shunted junction (RSJ) model with shunting resistor R_J , capacitance C , and critical Josephson current I_0 . In Fig. 1 an additional contact resistance R_G between the junction and the ground is also introduced. Let us consider first only the weak link alone. The dissipative Lagrangian of the RSJ circuit may be written as¹⁴

$$\mathcal{L} = \frac{1}{2} \left[\frac{\hbar}{q} \right]^2 c \dot{\theta}^2 - \frac{\hbar}{q} Q \dot{\theta} + \frac{\hbar}{q} I_0 \cos \theta + \left[\dot{Q} - \frac{\hbar}{q} \frac{1}{R_j} \dot{\theta} \right] \Phi, \quad (1)$$

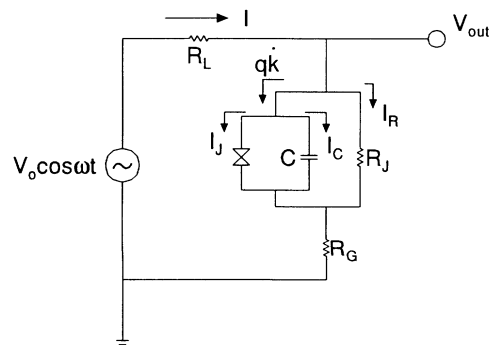


FIG. 1. Schematic diagram of the measurement circuit.

where $q = 2e$ is the charge of the Cooper pairs, θ denotes the Josephson phase difference across the junction, R_J is the shunting resistance, and \dot{Q} may be identified as the current I shown in Fig. 1. Equation (1) was derived through trial and error, since, when Q and θ are chosen as the two canonical variables, it gives rise to, respectively, the following Lagrangian equations of motion

$$\dot{\Phi} = -\frac{\hbar}{q}\dot{\theta} \quad (2)$$

and

$$\frac{\hbar}{q}C\ddot{\theta} + I_0\sin\theta - \frac{1}{R_J}\dot{\Phi} = \dot{Q}. \quad (3)$$

Therefore, $\dot{\Phi}$ may be identified as the time rate of flux change leaking across the junction, which, via Faraday law, is the negative of the voltage across the junction. Equation (2) and (3) are generally known as Josephson equations and the Josephson current is

$$I_J = I_0\sin\theta. \quad (4)$$

The canonical momenta conjugate to θ and Q are therefore

$$p_\theta = \frac{\partial\mathcal{L}}{\partial\dot{\theta}} = \hbar N = \frac{\hbar}{q} \left[C\frac{\hbar}{q}\dot{\theta} - Q - \frac{1}{R_J}\Phi \right], \quad (5)$$

$$P_Q = \frac{\partial\mathcal{L}}{\partial\dot{Q}} = \Phi. \quad (6)$$

As previously discussed, it is possible to employ a Routhian technique to separate the complete circuit into a quantum object and a classical apparatus. Thus, the Routhian Hamiltonian operator may be derived from the Lagrangian of Eq. (1) using the following

$$\mathcal{R} = \dot{\theta} \frac{\partial\mathcal{L}}{\partial\dot{\theta}} - \mathcal{L} = \frac{1}{2C} \left[qN + Q + \frac{1}{R_J}\Phi \right]^2 - \frac{\hbar}{q}I_0\cos\theta - \dot{Q}\Phi, \quad (7)$$

and the Routhian \mathcal{R} may be partitioned as the Hamiltonian of the conservative system consisting of an ideal Josephson junction and a shunting capacitance by redefining the term inside the bracket. Thus, p_θ shall be replaced by the operator $-i\hbar(\partial/\partial\theta)$ and the system possesses discrete quantum levels specified by

$$\mathcal{R} \left[\theta, \frac{\partial}{\partial\theta}; Q, \dot{Q} \right] \psi_n(\theta) = \Lambda_n(Q, \dot{Q}) \psi_n(\theta), \quad (8)$$

and Λ_n is the effective Lagrangian generated by \mathcal{R} for apparatus measurements. At this stage one may justify the definition of N in Eq. (5). The time dependence of N may be obtained from the commutation relation or

$$\dot{N} = \frac{i}{\hbar}[\mathcal{R}, N] = -\frac{I_0}{q}\sin\theta \quad (9)$$

and

$$\dot{\theta} = \frac{i}{\hbar}[\mathcal{R}, \theta] = \frac{q}{\hbar} \frac{1}{C} \left[qN + Q + \frac{2}{R_J}\Phi \right], \quad (10)$$

which reduce to Eqs. (4) and (3) if we identify the Josephson current I_J as

$$I_J = -q\dot{N}. \quad (11)$$

$\Lambda_n(Q, \dot{Q})$ is the Lagrangian operator treated classically and it is a function of R_J . As such, $\Lambda_n(Q, \dot{Q})$ obeys the classical relationship

$$\frac{\partial}{\partial t} \left[\frac{\partial\Lambda_n}{\partial\dot{Q}} \right] = \frac{\partial\Lambda_n}{\partial Q}. \quad (12)$$

Equations (8) and (12) totally specify the dynamics of the system. We rewrite Eq. (8) in the following form

$$\left\{ \left[-i \left[\frac{\partial}{\partial\theta} \right] + k \right]^2 - v_0\cos\theta \right\} \phi_n(\theta) = W_n(k) \psi_n(\theta) \quad (13)$$

or

$$\mathcal{H}(k) \psi_n(\theta) = W_n(k) \psi_n(\theta).$$

The operator \mathcal{H} is similar to \mathcal{R} except we introduce the following definition

$$v_0 = 2C\hbar I_0/q^3, \quad (14)$$

$$qk = Q + \frac{\Phi}{R_J}, \quad (15)$$

and W_n is related to Λ_n by

$$\Lambda_n(Q, \dot{Q}) = \dot{Q}\Phi - \frac{q^2}{2C} W_n \left[Q + \frac{\Phi}{R_J} \right]. \quad (16)$$

Equation (16) connects that which is excited quantum mechanically and that which is measured by the apparatus. From Eq. (12) we have,

$$\dot{\Phi} = -\frac{q}{2C} \frac{dW_n(k)}{dk}, \quad (17)$$

and, therefore, the voltage across the junction, $-\dot{\Phi}$, can be computed if $W_n(k)$ is known as a function of k , Eq. (13). We note that the resistance R_J enters the equation of motion, Eq. (17), as a Lagrangian multiplier in Eq. (16). The current flowing across resistor R_J is

$$I_R = -\frac{\dot{\Phi}}{R_J}, \quad (18)$$

and Eq. (15) implies

$$I = \dot{Q} = q\dot{k} + I_R = q\dot{k} - \frac{\dot{\Phi}}{R_J} = q\dot{k} + \frac{q}{2R_J C} \frac{dW_n(k)}{dk}. \quad (19)$$

Let us now consider the entire circuit of Fig. 1. Applying Kirchhoff's law, we have

$$V_0\cos\omega t = IR_T + I_R R_J, \quad (20)$$

where $R_T = R_L + T_G$. When Eq. (19) is used, Eq. (20) can be written as

$$\dot{k} = k_0\cos(2\pi\tau) - b_0 \frac{dW_n(k)}{dk}, \quad (21)$$

where

$$k_0 = V_0 / (\omega R_T q),$$

$$b_0 = 1 / (2CR_{\parallel}\omega),$$

$$R_{\parallel} = 1 / (1/R_T + 1/R_J).$$

In Eq. (21) normalized time τ has been used and $\tau = t/T = \omega t / 2\pi$. The output voltage in Fig. 1 is

$$V_L = IR_G + \frac{q}{2C} \frac{dW_n(k)}{dk} \\ = \omega q R_L \left[r_G k_0 \cos(2\pi\tau) + \frac{r_J b_0}{1 + r_G + r_J} \frac{dW_n(k)}{dk} \right], \quad (22)$$

where r_G and r_J are given by $r_G = R_G/R_L$ and $r_J = R_J/R_L$.

RESULTS

The wave function of the Cooper pair is periodic in θ so that $\psi_n(\theta + 2\pi) = \psi_n(\theta)$. One may express $\psi_n(\theta)$ as

$$\psi_n(\theta) = \sum_{m=-\infty}^{\infty} a_{mn} e^{im\theta}, \quad (23)$$

where $n=0$ designates the wave function of the ground state, $n=1$ is the first excited state, $n=2$ is the second excited state, and so forth. Substituting Eq. (23) into Eq. (13), multiplying both sides of Eq. (13) by $e^{-im'\theta}$ and integrating both sides from $\theta=0$ to 2π , one obtains the following

$$\sum_{m'=-\infty}^{\infty} H_{mm'}(k) a_{m'n} = W_n(k) a_{mn}, \quad (24)$$

where $H_{mm'}(k)$ is the matrix element of $\underline{H}(k)$ defined as

$$H_{mm'}(k) = 2\pi \left[(m+k)^2 \delta_{m,m'} - \frac{\nu_0}{2} (\delta_{m,m'+1} + \delta_{m,m'-1}) \right]. \quad (25)$$

Therefore, $W_0(k)$ is the lowest eigenvalue of the matrix $\underline{H}(k)$, $W_1(k)$ is the next lowest eigenvalue, and so forth. $W_0(k)$, $W_1(k)$, and $W_2(k)$ have been plotted in Fig. 2 as functions of k for three ν_0 values, $\nu_0=0$, 0.2, and 0.5. Figure 2 resembles the energy band structure in the reciprocal k space for solids possessing translational symmetry. In this case we have instead the requirement that $W_n(k+p) = W_n(k)$ for any integer p , the Brillouin zone structure, since the potential energy in Eq. (13), $\nu_0 \cos\theta$, is periodical in θ . The splitting between bands depends on the magnitude of the potential. The larger the ν_0 value, the larger is the splitting between the bands. The periodical structure of the $W_n(k)$ energy bands corresponds to add/remove integer number of Cooper pairs to/from the conservative system consisting of the Josephson junction and the capacitor.

We show in Fig. 3 plots of dW_n/dk as a function of k for the ground state ($n=0$) for several ν_0 values.

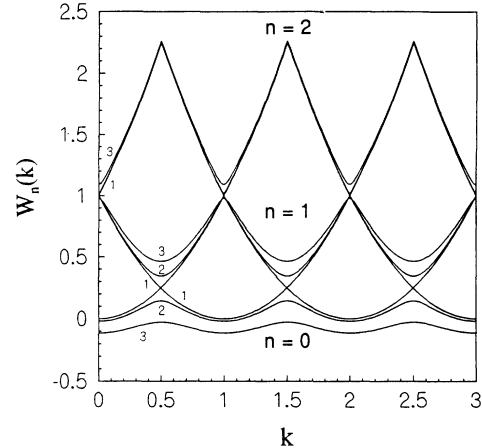


FIG. 2. Energy band structures of the weak-link system for the ground state ($n=0$), first excited state ($n=1$), and second excited state ($n=2$). (1): $\nu_0=0$, (2): $\nu_0=0.2$, (3): $\nu_0=0.5$.

dW_n/dk relates directly to the junction voltage, see Eq. (17), which can be compared directly with measurements. In Fig. 3 it is seen that the amplitude of dW_0/dk decreases with increasing ν_0 . Therefore, quantum effects may be enhanced by minimizing the product of I_0 and C . Both quantities depend on the detail fabrication of a weak link. From dW_n/dk , $k(t)$ can be integrated numerically using Eq. (21), and the output voltage can then be calculated from Eq. (22). We have used a fourth-order Runge-Kutta algorithm in double precision arithmetic in the integration of Eq. (21). Since Eq. (21) is a first-order differential equation, the initial value of k is unknown, $k(0)$. Detailed examination of $k(t)$ on $k(0)$ revealed that the steady-state solution of $k(t)$ is insensitive to $k(0)$. As such, we have arbitrarily chosen the initial value of k to be $k(0)=0$, since we were interested only in steady-state solutions of $k(t)$.

We have fabricated weak links of high- T_c films on single grain boundaries. One-to-one photolithography was

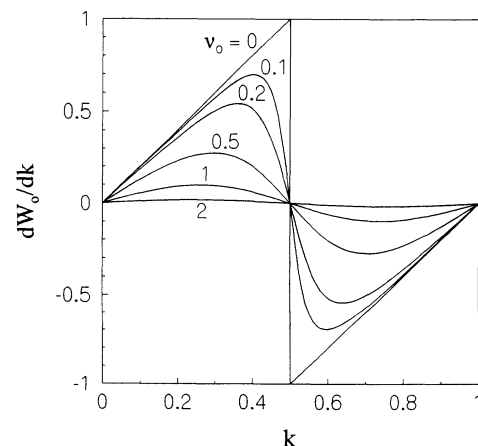


FIG. 3. Derivative of the energy band of the ground state ($n=0$) shown in Fig. 2.

used to make bridges across the grain boundary of the substrate. The typical dimension of the bridges as $20 \times 40 \mu\text{m}$. The critical current of the bridge was about $50 \mu\text{A}$ and the transition temperature about 81 K. By shining microwave radiation at 21 GHz onto the link, the usual Shapiro steps were found on the V - I characteristics. Sinusoidal signals were applied to the weak link bridge and it was monitored simultaneously with the output voltage signals across the weak link bridge. Figure 4 shows the output nonlinear voltage signal of the weak link junction at 40 K where the input frequency was 1.8 MHz and the peak-to-peak input voltage was 1 V. In Fig. 4 the theoretical curve is also shown together with the measured output voltage. In the calculation the following parameters were used: $\nu_0=0.2$, $k_0=2$, $b_0=2$, $r_J=0.02$, $r_G=0.01$, and $n=0$ (the ground state). We believe that there is general agreement between theory and experiment.

We now discuss the nonlinear ac response of the weak-link junction. The voltage signal in Fig. 4 is a result of a fine-structure signal superimposed on the fundamental signal. The fundamental signal is the drive frequency of the source. The fine structure results from the band structure of the quantum states shown in Fig. 2. In Fig. 4 it is seen that there are six fine structures over one period of the input signal. This implies that the amplitude of $k(t)$, k_0 in Eq. (21), covers three Brillouin zones in each half cycle of sweep of the input signal. Since R_L used was 100Ω and, from dc measurements of the weak link junction, $I_0 \approx 0.3 \mu\text{A}$ and $R_T = R_G + R_J \approx 3 \Omega$, it implies that $R_J \approx 2 \Omega$ and $R_G \approx 1 \Omega$. The shunting capacitance is calculated to be 10^{-16} F from Eq. (14), a value which can be estimated from calculating the Coulomb energy between crystallites in the film. Distance between crystallites is estimated to be about 2000 \AA .

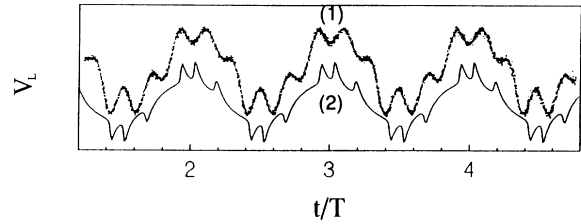


FIG. 4. Comparison between theory (curve 2) and experiment (curve 1) for the load voltage at 1.8 MHz. The peak-to-peak input voltage was 1 V and the abscissa has been normalized with respect to one period of the driving signal T . Theoretical curve was derived by plotting Eq. (22) using the solution of Eq. (21); $\nu_0=0.2$, $k_0=2$, $b_0=2$, $r_J=0.02$, $r_G=0.01$, and $n=0$.

CONCLUSION

Macroscopic quantum effects have been observed on a YBCO grain-boundary weak link. The theory clearly distinguishes the quantum object from the classical apparatus, enabling us to interpret the quantum measurements in a classical manner. The theoretical formulation may be applicable to any circuit containing a Josephson junction and a measuring apparatus represented by a loss or dissipation in the circuit. The nonlinear response induced in this microwave measurement may be attributed to the band structure of the junction weak link. We have observed the ground state of the charge mode. We estimate that the minimum separation in GHz between the ground and first excited state is about 150 GHz based upon our estimate of C in our circuit.

ACKNOWLEDGMENT

We wish to thank NSF for sponsoring this research.

¹H. Huang, H. Jiang, A. Widom, and C. Vittoria, IEEE Trans. Magn. **MAG-28**, 226 (1992).

²M. T. Tuominen, J. M. Hergenrother, T. S. Tighe, and M. Tinkham, Phys. Rev. Lett. **69**, 1997 (1992).

³R. V. Voss and R. A. Webb, Phys. Rev. Lett. **47**, 265 (1981).

⁴W. den Boer and R. de Bruyn Ouboter, Physica (Utrecht) **98B+C**, 185 (1980).

⁵R. J. Prance *et al.*, Nature (London) **289**, 543 (1981).

⁶D. D. Awschalom, M. A. McCord, and G. Grinstein, Phys. Rev. Lett. **65**, 783 (1990).

⁷A. Widom, J. Low Temp. Phys. **37**, 449 (1979).

⁸A. O. Caldeira and A. J. Leggett, Phys. Rev. Lett. **46**, 211 (1981).

⁹A. O. Caldeira and A. J. Leggett, Ann. Phys. **149**, 374 (1983).

¹⁰A. J. Leggett, in *Proceedings of the 1983 NATO ASI on Percolation, Localization and Superconductivity* (Pergamon, New York, 1984).

¹¹A. J. Leggett, in *Proceedings of the International Symposium on the Foundations of Quantum Mechanics*, edited by S. Kammerfuchi (Tokyo, 1983), p. 74.

¹²R. de Bruyn Ouboter, in *Proceedings of the International Symposium on the Foundations of Quantum Mechanics* [11].

¹³H. Jiang, H. How, A. Widom, C. Vittoria, T. Yuan, and K. Char (unpublished).

¹⁴A. Widom, H. Jiang, T. Yuan, H. How, and C. Vittoria (unpublished).